Maximizing the displacement of compact planar dielectric elastomer actuators

Samuel Rosset[a,*], Oluwaseun A. Araromi[a], Herbert R. Shea[a]

[a] *Microsystems for Space Technologies Laboratory (EPFL-LMTS), Ecole polytechnique fédérale de Lausanne, Neuchâtel, Switzerland*

Abstract

We present a model and its experimental validation for the optimization of the in-plane displacement of a rigid platform mounted on a compact dielectric elastomer actuator. Unlike the situation in which the mechanical prestretch of the membrane is maintained by a dead load (which leads to the highest strain, but is unsuitable for most practical applications), we study here the case in which the dielectric membrane is stretched on a frame, with the passive zones of the membrane acting as non-linear springs, thus avoiding external weights or springs, hence allowing for a compact and simple device. We demonstrate how to maximize the displacement of the platform relative to the overall size of the device by optimum choice of membrane prestretch and electrode geometry. In particular, we show that using a passive membrane decreases the maximum displacement of the platform by a factor of 2 compared to constant-force case. However, this loss can be compensated by using bidirectional actuation, with electrodes on both sides of the platform (one side at a time serving as the passive membrane). The differences between the idealised situation of the model and manufacturable devices are discussed and validated by finite element model simulations and experimental measurements.
 Link to publisher version: 10.1016/j.eml.2015.04.001

Keywords: dielectric elastomer actuators, soft actuators, large displacement, non-linear materials, silicone

1. Introduction

Dielectric elastomer actuators (DEAs) are soft transducers formed by a thin elastomeric layer sandwiched between two compliant electrodes, and capable of exhibiting large strains (from 10% to above 1000%) compared to other actuation technologies[1, 2]. When a voltage is applied between the electrodes the generated electrostatic force squeezes the dielectric, causing a decrease in thickness

*Corresponding author

Email addresses: samuel.rosset@a3.epfl.ch (Samuel Rosset), seun.araromi@epfl.ch (Oluwaseun A. Araromi), herbert.shea@epfl.ch (Herbert R. Shea)

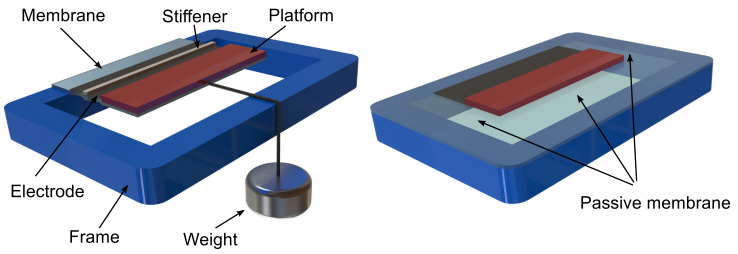

Figure 1: Left: Direct application of the dead weight approach with anisotropic prestretch to optimize the in-plane displacement of a moveable platform. Right: Realistic implementation of an actuator designed to move a platform in the plane of the membrane. The stretched membrane covers the complete frame, and the weight is consequently replaced by a passive zone of the membrane.

and increase in surface area[1]. This basic actuation principle has been exploited in many different configurations. For example, the expansion of the surface of the electrodes can be used to cyclically stretch biological cells[3], or modify the period of a tuneable optical diffraction grating[4]. When several layers are piled to form a stack actuator, the thickness compression effect can be used in devices that compress upon activation, similar to natural muscles[5, 6], or the combination of a stretched DEA and a flexible frame can lead to out-of-plane bending in a configuration known as a dielectric elastomer minimum energy structure[7, 8]. Finally, another interesting configuration consists in using the expansion of the electrodes to move a rigid object fixed on the membrane, thus providing a displacement of the platform in the plane of the membrane. This principle is used in different applications, such as Optotune's Laser Speckle Reducer[9], Artificial Muscle's haptic feedback technology[10], or a mm-wave RF phase shifter developed at EPFL[11]. For all these applications, it is highly desirable to minimize the overall size of the device, given a required displacement.

In this contribution, we show how to optimize the displacement of a moving rigid platform attached to a DEA by using the non-linear mechanical properties of the elastomeric membrane. The objective consists in maximizing the displacement of the platform relative to the overall size of the device, in order to obtain a large displacement in a small package. In particular, we study the situation in which the dielectric membrane is stretched over a frame and separated in active zones (zones covered by electrodes) and passive zones acting as non-linear springs. This configuration corresponds to the real-world applications mentioned above, but differs from the ideal situation in which the mechanical prestretch of the membrane is maintained by a dead load, and which has been shown to lead to the largest actuation stretches[12, 13].

Lu et al. have studied the use of a dead weight and different prestretch conditions to optimize the stretch of a strip-like actuator[13]. They have shown that the stretch of the actuator was maximized when a high prestretch value was applied in the width of the strip (i.e. perpendicular to the actuation direction),

while a low-value prestretch is applied in the actuation direction and maintained by a dead weight. The high prestretch in the transverse direction is sustained by stiff fibres fixed on the membrane. An idealized literal application of the optimized configuration identified by Lu et al. to the in-plane displacement of a rigid platform is shown in figure 1 left: a prestretched piece of elastomeric membrane is attached to a frame at one extremity, and to a platform at the other extremity. The prestretch in the actuation direction is maintained by a dead load, and the prestretch in the transverse direction is maintained by the anchor points of the membrane to the frame and to the platform, as well as by additional stiffeners fixed on the membrane if needed. Stiffeners are used to keep the width/length ratio of the suspended part of the membrane to a value larger than 5, in order to avoid a too large relaxation of the prestretch through necking. However, there are limitations to this implementation for real-world devices. For example, the use of dead load is highly impractical, as the devices must generally be able to work in any orientation, and attaching the weights to the actuators is not compatible with large-scale manufacturing. In addition, prestretching small elastomer membranes and fixing them on frames are difficult operations, especially for miniature devices. Generally, prestretching is done by mechanically stretching a larger membrane, on which frames are subsequently fixed. The membrane covers the complete frame, and therefore presents fixed boundary conditions on every edge of the frame opening.

Consequently, a more realistic implementation of an actuator made to displace a platform in the plane of the membrane consists of a membrane stretched over an opening in a frame, with a rigid platform fixed to its surface (figure 1 right). This configuration presents two major differences compared to the situation modelled by Lu et al. in their work (figure 1 left)[13]: a) there is passive membrane on the sides of the platform and electrodes, and b) the constant force provided by the dead load is replaced by a region of the membrane which is passive (not covered by electrodes). The side membrane issue can be solved by two different methods: either the frame opening can be made much wider than the platform to increase the size of the passive lateral region (but at the cost of a larger device), or the membrane can be post-processed, cutting the membrane on the sides in order to free the platform. We have developed a process flow demonstrating the latter using a CO_2 laser to selectively cut precise regions of the suspended membrane, as detailed in [14]. This approach involves a longer production process, but allows to limit the width of the overall device. More information on the impact of the passive membrane on the sides is given in section 2.4 of this paper. The passive region issue is more problematic, as unlike a dead load, it does not provide a constant force on the platform, but a force which is going to decrease with the displacement of the platform, thus causing a reduction of the actuator strain, compared to the constant force situation.

In the following sections, we present an analytical model in order to analyse the impact of the replacement of the dead load by an elastomeric membrane (i.e. a strain-dependent non-linear spring), and we use it to identify the best actuator geometry and prestretch conditions that maximize the displacement of the devices relative to their size. We then use finite element model (FEM) simu-

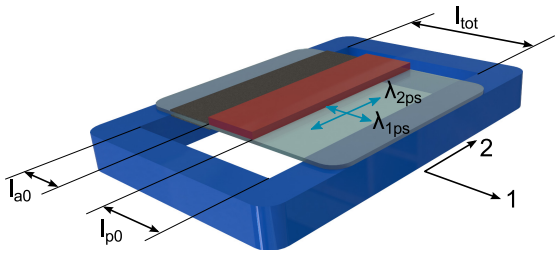

Figure 2: Geometry used for the model. The membrane has a prestretch of λ_{1ps} and λ_{2ps} and is separated in 3 separate regions: an active region of length l_{a0} coated with compliant electrodes, a passive region of length l_{p0}, and a rigid platform separating the two zones.

lations to investigate the differences between the idealized situation used for the analytical model, and the more complex configurations encountered with real-world devices. Finally, we fabricate and characterize planar DEAs of the same geometry than used for the simulations, in order to perform an experimental verification of the models.

2. Analytical model

The geometry for the model is shown in figure 2: the membrane is pre-stretched on a frame with stretch ratio values of λ_{1ps} in direction 1 (actuation direction) and λ_{2ps} direction 2. The suspended part of the membrane is separated into three separate zones. There is an active zone of initial length l_{a0}, which is covered by electrodes and which represents the actuator part of the device, expanding when a voltage is applied. There is a passive zone of initial length l_{p0}, which acts as a non-linear spring, relaxing when the active part expends. Finally, there is a platform, considered infinitely stiff and weightless, fixed on the membrane and separating the active and passive zones. When a voltage is applied to the device, the active zone expands to a voltage-dependent length $l_a > l_{a0}$, and the passive zone contracts to a length $l_p < l_{p0}$, causing the platform to move by $\Delta l_a = l_a - l_{a0}$ (figure 3). It is supposed that a post-processing step has been performed to cut the membrane on both sides of the electrodes, platform and passive zone. The total length of the free suspended membrane (l_{tot}) is the addition of the length of the active and passive zones, as well as the length of the platform. Although not represented in the figure, stiffeners may need to be added to the active and passive zones in order to keep the width/length aspect ratio to a value higher than 5, in order to prevent prestretch relaxation in direction 2. If stiffeners are used, their lengths must be added to the total device length l_{tot}. Because the platform acts as an infinitely rigid body which is shifted (but not deformed), its length has no influence on the behaviour of the device, and to simplify, we consider a zero-length platform for the analytical model, such as $l_{tot} = l_a + l_p$. The width of the device w does not influence the strain, but should be chosen sufficiently large to avoid necking

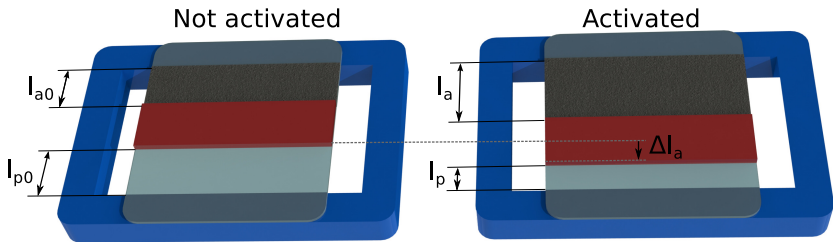

Figure 3: Actuation principle. Left: equilibrium position at 0 V with active and passive zones of length l_{a0} and l_{p0}. Right: active position (>0 V). The active zones expands to $l_a > l_{a0}$, which causes the platform to move by $\Delta l = l_a - l_{a0}$

of the membrane and relaxation of the stress in direction 2 (or else stiffeners must be added).

The main parameters that need to be investigated in order to optimize the actuation are the prestretch in direction 1 and 2 (λ_{1ps} and λ_{2ps}), and the active ratio $r_a = l_a/(l_a + l_p)$, i.e. the length of the electrode compared to the total length of the suspended membrane. The mechanical properties of the elastomer membrane are represented by a strain energy density function w. Among the different hyperelastic strain energy density functions that can be used to model elastomers, we choose the Gent model for its ability to account for the rapid stiffening of the material past a maximal stretch, at which the stress diverges. According to the Gent model, the energy density stored into a piece of elastomer submitted to stretch is defined by[15]:

$$w = -\frac{\mu J_m}{2} \ln\left(1 - \frac{I_1 - 3}{J_m}\right), \tag{1}$$

where μ is the shear modulus of the elastomer, J_m a parameter that accounts for the finite elongation at break of the material, and I_1 the first invariant of the stretch tensor ($I_1 = \lambda_1^2 + \lambda_2^2 + \lambda_3^2$). At rest (i.e. without applied voltage), the stretch in both active and passive zones are equal to the prestretch values λ_{1ps} and λ_{2ps}, but when a voltage is applied to the electrodes, the equilibrium is shifted. Because of the constrained geometry in direction 2, we assume no expansion in this direction, which means that the stretch in direction 2 of the active zone λ_{2a} and in the passive zone λ_{2p} are equal to the membrane prestretch in direction 2 ($\lambda_{2a} = \lambda_{2p} = \lambda_{2ps}$) whatever the applied voltage. The stretch along direction 1 of the active zone is geometrically defined by:

$$\lambda_{1a} = \frac{l_a}{l_{a0}} \lambda_{1ps}. \tag{2}$$

Similarly, the stretch along direction 1 of the passive zone is given by:

$$\lambda_{1p} = \frac{l_p}{l_{p0}} \lambda_{1ps} = \frac{l_{tot} - l_a}{l_{tot} - l_{a0}} \lambda_{1ps} = \frac{l_{tot} - \frac{\lambda_{1a} l_{a0}}{\lambda_{1ps}}}{l_{tot} - l_{a0}} \lambda_{1ps}. \tag{3}$$

Because of geometric constraints, the stretch in the active and passive zone are linearly dependent, as shown by equation 3.

To find the equilibrium position of the actuator for a combination of the parameters λ_{1ps}, λ_{2ps}, r_a, and applied voltage V, we compute the elastic energy stored in the active and passive zones of the membrane, as well as the electrostatic energy stored into the active region for different values of λ_{1a}. We neglect the mechanical impact of the electrodes. The equilibrium position is found for the value of λ_{1a} leading to the smallest total energy. Based on equation 1, and using the volume conservation property of elastomers ($\lambda_1\lambda_2\lambda_2 = 1$), the mechanical strain energy stored into the active (E_{ma}) and passive (E_{mp}) zones is given by:

$$E_{ma} = w(\lambda_{1a}, \lambda_{2ps})V_a = -\frac{\mu J_m}{2} \ln\left(1 - \frac{\lambda_{1a}^2 + \lambda_{2ps}^2 + \lambda_{1a}^{-2}\lambda_{2ps}^{-2} - 3}{J_m}\right) w l_{a0} t_0 \quad (4)$$

$$E_{mp} = w(\lambda_{1p}, \lambda_{2ps})V_p = -\frac{\mu J_m}{2} \ln\left(1 - \frac{\lambda_{1p}^2 + \lambda_{2ps}^2 + \lambda_{1p}^{-2}\lambda_{2ps}^{-2} - 3}{J_m}\right) w l_{p0} t_0, \quad (5)$$

where V_a and V_p are the volumes of the active and passive zones, t_0 is the thickness of the membrane after the prestretch (that is the effective thickness of the membrane without any applied voltage), and λ_{1p} is given by equation 3. The electrostatic energy stored into the capacitance C formed by the active area when a voltage V is applied between the electrodes is given by:

$$E_{es} = -\frac{CV^2}{2} = -\frac{\epsilon\ l_a\ w\ V^2}{2t} = -\frac{\epsilon\ \lambda_{1a}^2\ l_{a0}\ \lambda_{2ps}\ w\ V^2}{2\lambda_{1ps}\ t_0}, \quad (6)$$

where ϵ is the permittivity of the elastomer and t is the thickness of the active zone in its deformed state. The total energy E_{tot} is calculated by summing the 3 different contributions:

$$E_{tot}(V, \lambda_{1a}) = E_{ma}(\lambda_{1a}) + E_{mp}(\lambda_{1a}) + E_{es}(V, \lambda_{1a}), \quad (7)$$

and for a given applied voltage V, the equilibrium stretch in the active region can be found by solving

$$\frac{\partial E_{tot}}{\partial \lambda_{1a}} = 0 \qquad \frac{\partial E_{tot}^2}{\partial \lambda_{1a}^2} > 0. \quad (8)$$

Doing so for different values of voltage allows to compute the stretch in the active zone as a function of voltage, which can then be divided by the prestretch in direction 1 in order to obtain the actuation stretch ratio λ'_{a1} which describes the expansion of the electrodes:

$$\lambda'_{1a}(V) = \lambda_{1a}(V)/\lambda_{1ps}. \quad (9)$$

The next step consists in defining what is the maximal actuation stretch that can be obtained for a combination of prestretch and active ratio. The actuation

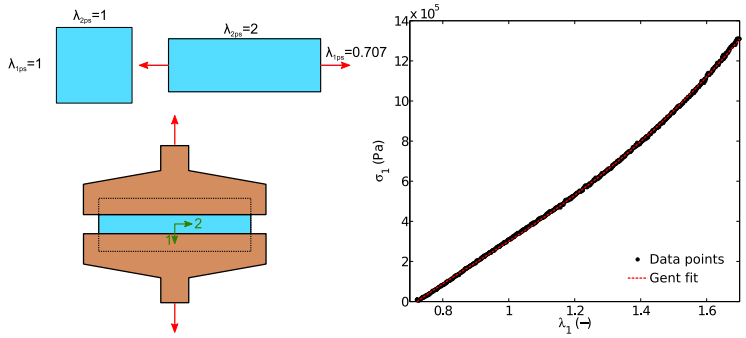

Figure 4: Left: Sample preparation for the pull-test experiment in pure shear mode, with a prestretch in direction 2. Right: Experimental pull test data in pure shear mode, with a prestretch in direction 2 of $\lambda_{2ps} = 2$. The fit with the Gent model leads to $\mu = 0.365$ MPa and $J_m = 16.6$.

stretch is indeed limited by different failure modes: dielectric breakdown and loss of tension. Dielectric breakdown happens when the electric field across the elastomer membrane exceeds a threshold value E_{bd} (either directly or through electromechanical instability which causes rapid thickness decrease of the membrane). Loss of tension of the membrane in direction 1 or 2 happens when the stress in direction 1 or 2 becomes negative (i.e. compressive). Because thin membranes can not sustain compressive stress, they buckle and ripple out of plane. In the direction of actuation, this causes the platform to move out of plane. The maximal achievable actuation stretch is the stretch obtained just before one of the above-mentioned failure modes is observed.

2.1. Gent hyperelastic model

To illustrate the model presented above, we apply it to the silicone elastomer Sylgard 186 from Dow Corning. We perform a pull-test on a sample of the elastomer, in order to obtain the two parameters of the model μ and J_m. It is generally assumed that a set of model parameters applies to a given material, irrespective of its shape, size, and state of deformation. However, in reality, the mechanical parameters of an elastomer generally depends on its aspect ratio (there are differences between a block and a very thin membrane), preparation method (curing temperature and time for example), and state of deformation. The later point is due to the Mullins effect, a stretch-induced degradation of the PDMS, which renders the mechanical properties of an elastomer dependent on the largest stretch it has seen[16], and which has a non-negligible impact on silicone elastomers[17]. Consequently, a more accurate estimation of the mechanical properties of an elastomer can be obtained if the mechanical test is performed on a sample of a geometry close to the final device, and in a similar stress condition. For this reason, our pull-test is performed in pure shear mode on a 45 μm-thick membrane. Because it is expected that the optimal prestretch in direction 2 for the devices will be high, we perform the pull test on a sample

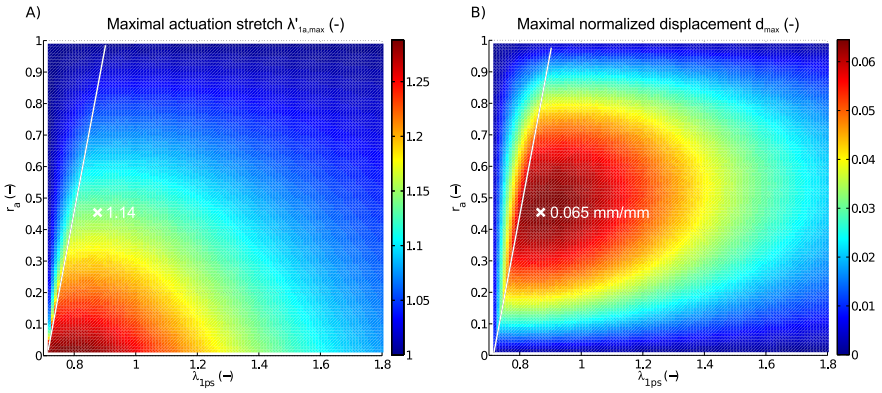

Figure 5: A) Maximal actuation stretch in the active zone $\lambda'_{1a,max}$ as a function of prestretch in actuation direction (λ_{1ps}) and active ratio r_a for a fixed prestretch in direction 2 $\lambda_{2ps} = 2$. The white line indicates the limit between two failure modes: loss of tension in direction 1 on the left and dielectric breakdown on the right. B) Maximal normalized displacement of the platform for the same parameters, showing an optimum active ratio $r_a = 0.46$ and prestretch $\lambda_{1ps} = 0.88$, at which a normalized displacement of 0.065 can be obtained. This corresponds to an actuation stretch of $\lambda'_{1a} = 1.14$

which is prestretched by a factor of two in the direction 2 (figure 4). To do so, a 45 μm Sylgard 186 membrane is prestretched uniaxially by a factor of 2 in direction 2 (and allowed to relax in direction 1 and 3 to a stretch ratio of $1/\sqrt{2}$). Then this prestretched membrane is fixed to a set of clamps so that the portion of the membrane which is stretched is much wider (100 mm) than long (10 mm), as this ensures that the stretch in direction 2 remains constant throughout the test. Figure 4 right shows the experimental data points, as well as Gent model fit. The Gent model presents a good fit to the experimental data, and leads to the following values for the model parameters: $\mu = 0.365$ MPa and $J_m = 16.6$.

2.2. Optimal active ratio r_a

As the first application of the model, we investigate the impact of the active ratio $r_a = l_a/(l_a + l_p)$, i.e. the length of the electrode compared to the total length of free membrane, and we compute the maximal actuation stretch $\lambda'_{a1,max}$ until failure (dielectric breakdown or loss of tension). For the graphical representation, we use Sylgard 186 elastomer using the Gent model parameters identified in section 2.1. The membrane is taken to be 25 μm thick after prestretch, and to have a relative permittivity $\epsilon_r = 2.5$. The maximum admissible field E_{bd} used to compute the maximal actuation stretch is chosen to be 100 V/μm, according to experimental results obtained previously[18]. This value corresponds to the breakdown of unprestretched Sylgard 186 membranes, and can be considered to be conservative, as the breakdown strength of elastomers generally increases with increasing prestretch[19]. Figure 5 left shows the value of $\lambda'_{a1,max}$ for a fixed prestretch in direction 2 of $\lambda_{2ps} = 2$, a prestretch in the actuation direction λ_{1ps} between $1/\sqrt{2}$ and 1.8, and an active ratio r_a

between 0 and 1. As the prestretch conditions correspond to the pull-test situation presented in section 2.1, the two Gent model parameters can be used with confidence. The maximal actuation stretch is $\lambda'_{a1,max} = 1.28$ and is observed for the smallest values of r_a and λ_{1ps}, which agrees with the findings of Lu et al. who have shown that the optimal situation consists in having a low constant force acting in the actuation direction[13]. Indeed, having a small active ratio r_a signifies that the stretch remains constant in the passive zone, thus effectively providing a constant force, and keeping the prestretch low in the actuation direction ensures that this pulling force is close to 0, just sufficient to avoid loss of tension. The maximal actuation stretch presents a ridge (indicated in the figure by a white line), which is caused by a change of failure modes: loss of tension in direction 1 on the left of the line, and dielectric breakdown on the right. Loss of tension in direction 2 and electromechanical instability do not occur, thanks to the prestretch in direction 2, which is sufficiently high to prevent these two failure modes.

Even though a small active ratio is the optimal situation to enhance the actuation stretch of the active zone, it is not necessarily the best configuration to optimize the displacement of the platform relative to the total size of the device. Indeed, a small r_a implies having a very long passive region, and therefore a large device. Or, if the size of the device is fixed, this means that the length of the active area is small: it will stretch much when activated, but being small, it will cause a small displacement of the platform. Consequently, the actuation stretch is not the most important parameter, if the ultimate goal is to optimize the displacement of the platform relative to the size of the device. We therefore define a normalized displacement d describing the displacement of the platform relative to the length of the active and passive zone:

$$d = \frac{\Delta l_a}{l_a + l_p} = \frac{l_{a0}\left(\lambda'_{1a} - 1\right)}{l_a + l_p} = r_a\left(\lambda'_{1a} - 1\right). \tag{10}$$

Figure 5 right shows the maximal normalized displacement for the same set of parameters. A maximal normalized displacement of 0.065 mm/mm is obtained for an active ratio of $r_a = 0.46$ and a prestretch in direction 1 of $\lambda_{1ps} = 0.88$, as indicated by the white cross. In this optimal configuration, the stretch in the active area is $\lambda'_{a1,max} = 1.14$, which is only half of the stretch that can be expected from a constant-force case. This shows that using a passive membrane to provide a pulling force on the platform instead of a dead weight has an important impact on the actuation stretch of the device. However, this effect can be mitigated by the fact that the optimal active ratio is closed to 0.5. If the actuator is designed to have an active region of the same length than the passive region, then electrodes can also be applied to the passive region. This allows bi-directional actuation: a pair of electrodes is energized while the second one is not, thus acting as the passive zone. To move the platform in the other direction the role of the active/passive zone is swapped, thus effectively multiplying by two the displacement range of the platform. For the situation presented here, a normalized displacement up to 0.128 (± 0.064) can be expected for bi-directional actuation with $r_a = 0.5$.

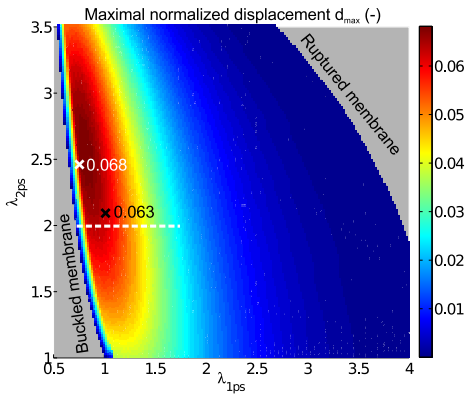

Figure 6: Maximal normalized displacement of the platform as a function of prestretch in directions 1 and 2 for an active ratio of 0.5. The maximal displacement of 0.068 is obtained for $\lambda_{1ps} = 0.76$ and $\lambda_{1ps} = 2.48$ as indicated by the white cross. The black cross indicates the optimal prestretch in a pure shear configuration. The two grey areas without data represent failure conditions at the prestretching step. The dashed white line represents the pull-test range used to extract the model parameters.

2.3. Optimal prestretch

With the active ratio r_a fixed at 0.5, it is now possible to optimize the prestretch in direction 1 and 2. The maximal normalized displacement of the platform is represented in figure 6 as a function of λ_{1ps} and λ_{2ps} for $r_a = 0.5$. It can be seen that in the case of Sylgard 186, the optimal prestretch situation is $\lambda_{1ps} = 0.76$ and $\lambda_{1ps} = 2.48$, leading to a normalized unidirectional displacement of 0.068 mm/mm. The grey zones in the figure represent the prestretch conditions for which the membrane is in a failure mode even before voltage is applied, either by loss of tension for too low values of prestretch, or by rupture of the membrane when the prestretch is too high. The dashed white line represents the stretch conditions during the pull test used to determine the two parameters of the Gent model. As discussed previously (c.f. section 2.1), the accuracy of the values presented on the graph decreases with increasing distance from the line.

The optimal configuration shown in figure 6 presents a major disadvantage: it lies on the edge of the loss-of tension in actuation direction failure mode, meaning that loss of tension occurs exactly at the maximal admissible electric field E_{bd}. This should be avoided, as it enables out-of-plane motion of the platform under its weight, due to the loss of tension of the membrane. In practice, it is preferable to design the actuator so that some tensile stress remains in the membrane when the maximal driving field is reached. This can be accomplished by slightly increasing the prestretch in direction 1, for example to a value of $\lambda_{1ps} = 1$ (i.e. in pure shear), which also presents the advantage of being easier to realize, as one dimension of the membrane remains constant during the prestretching process. The black cross in figure 6 indicates the optimal situation for pure shear prestretch: $\lambda_{1ps} = 1$, and $\lambda_{2ps} = 2.18$ for a maximal normalized

displacement of 0.063, and away from loss of tension.

2.4. Comparison of the analytical model with FEM simulations

The results presented in the previous sections are based on the ideal geometry of figure 2, in which there is absolutely no relaxation of the membrane along direction 2, and the membrane is cut at the exact same width than the platform. However, this geometry presents two practical limitations: Even with a large width/length aspect ratio maintained by stiffeners, part of the prestretch in direction 2 will relax through necking of the membrane, thus creating an inhomogeneous prestretch in the membrane. Secondly, it is necessary not to cut the membrane right at the border of the electrodes, in order to avoid electrical arcing in air between the two electrodes. A realistic device is shown in figure 7 A, with partial relaxation of the prestretch in direction 2, and a spacing of width s between the edge of the electrode and the edge of the membrane. To study the impact of the passive border of width s, we use finite element model (FEM) simulations in ANSYS (ANSYS Inc). The geometry of the simulated actuator consists of a 4-mm-long electrode, a 4-mm-long platform, and a 4-mm-long passive zone. These three regions are 30 mm wide, in order to provide a large width over length ratio of 7.5 for the passive and active region. A passive zone of width s is located on both sides of the device. The elastomer is chosen to be Sylgard 186, with the mechanical properties from section 2.1 and is equi-biaxially prestretched by a factor of 1.2. In a first step of the simulation, the prestretch is allowed to relax in the suspended portions of the membrane, and in a second step, the electrostatic pressure is added as a surface load to the active area, causing displacement of the platform. This last step is iterated several times, each time recalculating the electrostatic pressure to account for the reduction of the thickness of the membrane in the active zone, until the solution converges to a stable displacement (figure 8). A nominal field of 100 V/μm is used for the simulations, to match the maximal field E_{bd} used for the model.

The displacement of the platform obtained through the FEM simulations is normalized by the displacement calculated with the analytical model for the idealized geometry of figure 2. The blue curve of figure 9 shows the normalized displacement as a function of the lateral passive width s. Even for a zero-width lateral passive zone, one observes a smaller displacement compared to the analytical model (blue cross). This is due to the partial relaxation of the prestretch in direction 2 in the suspended zones: the assumption made in the analytical model that the stretch in direction 2 is constant and always equal to the prestretch value in this direction ($\lambda_{2a} = \lambda_{2p} = \lambda_{2ps}$) is a simplification compared to what is practically observed. Then, for increasing lateral passive width, the displacement decreases, due to the additional strain energy that must be stored into these lateral passive regions. As mentioned earlier, the lateral passive zone is necessary to avoid arcing between the top and bottom electrodes when the high driving voltage is applied. Based on our experience, it is necessary to leave at least 1 mm of gap per kV of applied voltage. With membrane thickness typically between 25 μm and 50 μm, a spacing s between 2.5 mm and

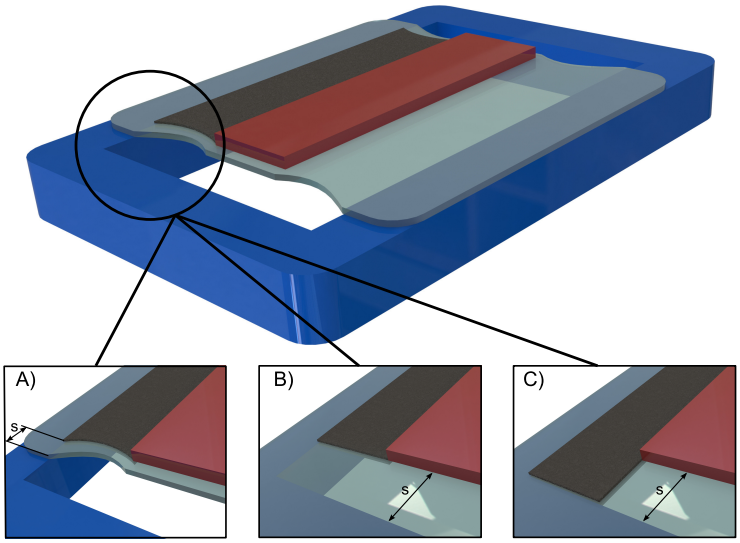

Figure 7: Various realistic configurations that differ from the analytical model: A) Membrane cut on the sides, but a gap s of membrane is left on each side to prevent arcing between the electrodes. B) Same situation as presented in sections 2.2 and 2.3, but the membrane is not cut. There is a gap s between the moving platform and the edge of the frame. C) Same situation as for B, but the electrode is extended to the edge of the frame.

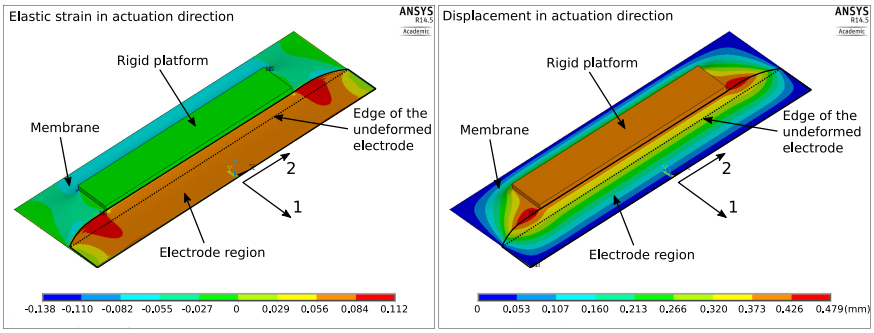

Figure 8: Simulation results for the case with extended electrodes (configuration C from figure 7), 100 V/μm of applied electric field, and 5 mm of spacing between the platform and the edge. Left: elastic strain in the actuation direction. Right: absolute displacement in the actuation direction.

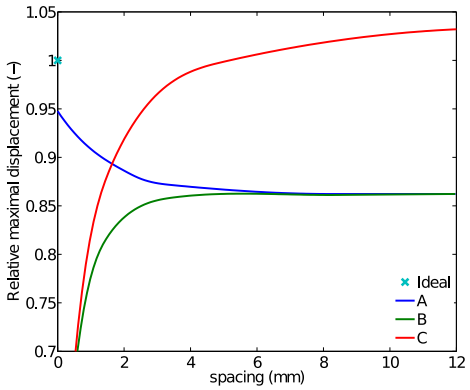

Figure 9: Maximal displacement of the platform as a function of the spacing s for the 3 cases shown in figure 7. The displacement is obtained by FEM simulations and normalized relative to the displacement predicted by the analytical model (which is indicated by a blue cross).

5 mm is necessary, thus effectively reducing the platform displacement to about 87% of what the analytical model predicts.

Because it is necessary to have lateral passive zones to prevent arcing, these passive zones can be extended and fixed to the border of the frame (figure 7 B), with a spacing s between the platform and the attachment point. This approach is very interesting from a fabrication point of view, as it removes the need for the membrane-cutting post-processing step, as well as the need for stiffeners, and corresponds to the situation shown in figure 1 right. The fact that the membrane is fixed to the frame on the sides is expected to have a negative impact on the displacement: on one hand, if the spacing s is reduced to 0, then no movement is possible, and when s becomes very large, the impact on displacement should be the same than for case A with a large values of s. FEM simulations similar to what is described above have been performed for configuration B and are reported in figure 9 (green curve). As predicted, a small spacing between the platform and the frame locks the displacement, but the impact of the border quickly saturates to 86% of the optimal displacement, for a spacing larger than 3.5 mm. Keeping in mind that even with a cut membrane (configuration A), a lateral passive zone of at least 2.5 mm is needed, the difference in displacement between situation A and B is negligible, and not worth the extra steps needed to cut the membrane once the electrodes and platform are applied.

Finally, as we have previously concluded that cutting the membrane is not necessary, an extra step can be taken, and the electrode can be extended up to the border of the frame, as depicted in figure 7 C. This configuration is expected to be closer to the analytical model, as the electrode is physically prevented from expanding along direction 2 by the edges of the frame, whereas in situations A and B, some energy is used in the deformation of the electrode in direction 2. The results of the simulation for configuration C is represented by the red line in figure 9. Similar to case B, a very small spacing between the platform and the frame prevents the displacement, but with increasing spacing s, the relative

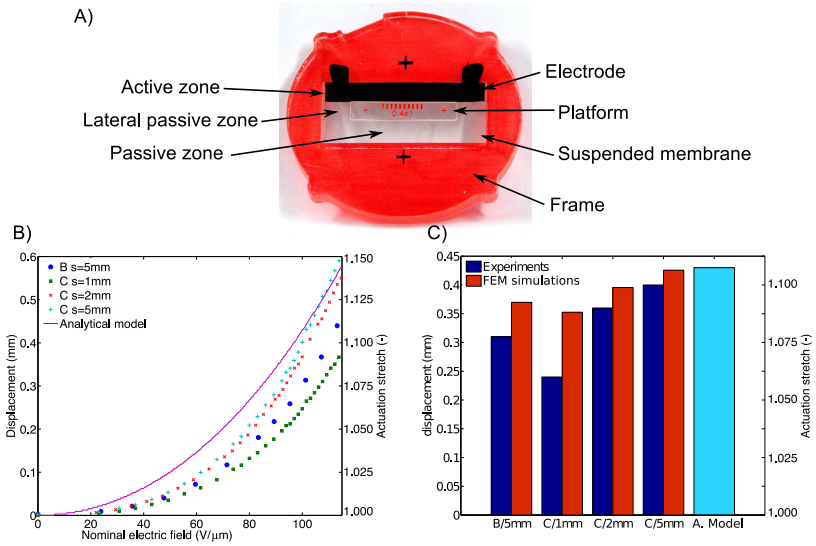

Figure 10: A) Picture of the actuator (design C, s=5 mm) used for the experimental verification. B) Measured displacement of the platform and actuation stretch of the electrode versus applied field for 4 actuators with different configurations, as well as predicted displacement from the model. C) Displacement of the platform and actuation stretch of the electrode at a driving electric field of 100 V/μm for the 4 different configurations, together with the respective results from the FEM simulations. The notation B/5mm means design B, s=5 mm, etc. The value predicted by the analytical model is also shown (A. Model).

displacement quickly rises up to the value predicted by the analytical model, which is obtained for $s = 0.5$ mm. For larger spacing values, the displacement even raises above the analytical model, due to the fact that on the sides, where there is no platform, the effective length of the actuator is larger, as the passive zone is twice longer.

3. Experimental verification

To verify the results of the simulations presented in section 2.4, actuators with the same geometry as for the FEM simulations are fabricated (figure 10 A). Thin Sylgard 186 membranes are cast and equi-biaxially prestretched to a factor of 1.2 to match the simulation conditions. The thickness of the prestretched membranes lies between 32 μm and 34 μm. The electrodes consist of a mixture of carbon black in silicone elastomer with a 1:10 weight ratio and are applied on the silicone membrane by pad printing before being cross-linked in an oven for 30 minutes at 80 ^{0}C. The moving platform is made in a 3 mm-thick Poly(methyl methacrylate) (PMMA) plate covered by a silicone dry adhesive on one side, and cut to the desired dimensions with a laser cutter. Then, the protective layer of the adhesive is removed, and the platform manually adhered at the centre of the membrane.

4 different geometries are made: configuration B with a 5 mm spacing between the platform and the border, and configuration C with spacings of 1 mm, 2 mm, and 5 mm between the platform and the border of the frame. The displacement of the platform as a function of applied electric field is measured with an automated setup consisting of a controlled high voltage source, a calibrated camera and image processing routines that allow tracking the displacement of the platform with a resolution of 3 μm (figure 10 B). The measurement clearly shows the impact of the different designs and of the spacing between the platform and the border of the frame. For example, with an equal spacing of 5 mm, larger displacements can be obtained for geometry C, for which the electrodes extend up to the frame border. The displacement of the actuators measured at a nominal field of 100 V/μm is shown in figure 10 C alongside the predicted displacements obtained by the FEM simulations and the analytical model. There is a good agreement between the measured values and the simulations, with a displacement approaching the value predicted by the model for the geometry C with 5 mm spacing. The smaller displacement observed for the actuator with the smallest spacing (1 mm) is probably due to a slight misalignment of the moving platform on the membrane which was not perfectly centred. Although the misalignment due to fabrication imprecision is expected to be identical on all the actuators, it has much more influence for low spacing values, as the impact of the passive zone is inversely proportional to the spacing. This hypothesis has been verified by simulating the effect of a platform placed on the membrane with a 500 μm offset along direction 2. For a spacing s of 5 mm, the effect of the offset is negligible, and the platform displacement reaches 98.8% of the expected value of a perfectly aligned platform. However the impact of alignment error increases for decreasing lateral passive zone width, and for $s = 1$ mm, an offset of 500 μm allows to reach only 76% of the expected displacement, i.e. 0.27 mm instead of the 0.35 mm shown in figure 10 C, and therefore much closer to the experimental value.

It can be seen that all of the tested actuators were able to withstand electric fields higher than the maximal value of 100 V/μm used to compute the maximal displacement for the analytical model and the simulations. In fact, the effective breakdown field observed on the actuators was between 115 and 120 V/μm. However, 100 V/μm can be defined as a safe-operating field for Sylgard 186, at which the actuator is expected to exhibit a long life time. The maximal displacement at breakdown has been observed on the actuator with the C configuration and the spacing of 5 mm: 0.67 mm for a field of 120 V/μm, corresponding to an actuation stretch of the electrode of 1.17.

4. Discussion

Although in a first approximation the behaviour of dielectric elastomer actuators can appear to be simple, with thickness compression proportional to the square of the applied field and inversely proportional to the Young modulus of the elastomer[1], real devices exhibit more complex behaviour due the non-linear stretch-stress mechanical characteristic of elastomers, the coexistence of passive

and active zones on the same device, as well as boundary conditions. For the particular case studied in this contribution, a simplified analytical model shows that the active ratio r_a, and the prestretches in the 2 in-plane directions have a strong influence on the maximal displacement of the moving platform placed on the elastomer membrane. The optimal values of these parameters depend on the properties of the elastomer used as the dielectric membrane, particularly the strain energy density function and should be evaluated on a case by case basis. However, general guidelines can be given. The active ratio can be fixed to 0.5, which is anyway close to the optimum value and allows bidirectional actuation, with electrode pairs added on both sides of the platform, thus allowing to double the displacement of the device without changing its size. This is particularly important in the context of device miniaturization, where it is crucial to minimize the overall size of a device needed to achieve a defined displacement. The prestretch in direction 1 must be low. In theory, the optimal situation is when the internal stress in the actuation direction reaches 0 at the maximal driving field. However, this situation is not desirable for real-world devices, because the weight of the platform can deform the membrane, which would cause out-of-plane motion. Depending on the targeted application, it is important that the platform stays in the plane of the membrane, and it is therefore necessary to keep some tensile stress in the membrane even at the maximal field. There is therefore a trade-off between actuation performance and parasitic out-of-plane motion of the platform. The prestretch in direction 2 must have a moderate value relative to the elongation at break of the elastomer. Using the model with different values of J_m (to simulate materials with different elongations at break) shows that in the range of tested values ($5 \leq J_m \leq 30$), there is a linear relationship between the optimal prestretch in direction 2 and the elongation at break in case of uniaxial extension, with the optimal value of λ_{2ps} being 57% of the maximal elongation of the elastomer as given by the Gent model. Mathematically, this means that the optimal prestretch in direction 2 can be approximated by solving

$$(0.57\lambda_{2ps})^2 + \frac{2}{0.57\lambda_{2ps}} - 3 - J_m = 0, \tag{11}$$

this being valid only if the elastomer can be modelled accurately with Gent model over its complete stretching range.

The theoretical optimal configuration implies that a non-negligible amount of strain energy is stored in the membrane by the prestretch. This can cause several issues, such as difficulty of holding the membrane on the frame or greater risk of the membrane tearing in case of small mechanical defects in the frame. Consequently, it is often beneficial to sacrifice some of the displacement potential of the device for easier manufacturing and improved robustness, by decreasing the prestretch on direction 2 below the optimal value. This should be compensated by a slight increase of the prestretch along the actuation direction, in order to avoid loss of tension.

5. Conclusions

An analytical model is presented for a planar DEA device moving a rigid platform along one direction in the plane of the membrane. The model simulates the more realistic and practical version of the hanging mass approach used in other work, by using an antagonistic prestretched elastomer membrane separated in active and passive zones. Although the studied geometry is more adapted to real-world devices, it presents the disadvantage of having a stretch-dependent force acting on the active zone, instead of a constant force as when dead weights are used. This stretch-dependent counter force was shown to cause a reduction of the displacement of the platform by a factor of two or more, compared to the constant force case.

The outcome of our model shows that when the geometry of the actuator is correctly chosen (active and passive zones of equal size), the reduced displacement caused by the stretch-dependent force can be compensated by the possibility of having bi-directional antagonistic actuation. The model also points out the importance of prestretch, which must be low in the actuation direction, but high enough to prevent loss of tension, even at the maximal stretch. A simple empirical relationship was established for the optimal prestretch in the transverse direction, based on the Gent model.

Because the model geometry is a simplification of real-world devices, FEM simulations were used to study the deviation between the simplified analytical model and more complex situations, taking into account the prestretch relaxation in direction 2, the impact of passive zones on the sides, or fixed lateral boundary conditions. The FEM simulations show that cutting the membrane on the sides is generally not necessary, and that the loss of displacement caused by lateral passive zones can be compensated by an extension of the electrodes up to the border of the frame.

The model represents a precious design tool for the development of planar DEAs consisting of a stiff movable platform that is displaced along one direction.

6. Acknowledgments

The authors wish to thank the members of EPFL-LMTS for fruitful discussions and advice. This work has been partially funded by the Swiss National Science Foundation grant 200020-153122.

References

[1] R. Pelrine, R. Kornbluh, Q. Pei, J. Joseph, High-speed electrically actuated elastomers with strain greater than 100%, Science 287 (5454) (2000) 836–839. doi:10.1126/science.287.5454.836.

[2] C. Keplinger, T. Li, R. Baumgartner, Z. Suo, S. Bauer, Harnessing snap-through instability in soft dielectrics to achieve giant voltage-triggered deformation, Soft Matter 8 (2) (2012) 285–288. doi:10.1039/C1SM06736B.

[3] S. Akbari, H. R. Shea, An array of 100um x 100um dielectric elastomer actuators with 80% strain for tissue engineering applications, Sensors and Actuators A: Physical 186 (2012) 236 – 241. doi:10.1016/j.sna.2012.01.030.

[4] M. Kollosche, S. Doering, J. Stumpe, G. Kofod, Voltage-controlled compression for period tuning of optical surface relief gratings, Optics Letters 36 (8) (2011) 1389–1391. doi:10.1364/OL.36.001389.

[5] F. Carpi, C. Salaris, D. D. Rossi, Folded dielectric elastomer actuators, Smart Materials and Structures 16 (2) (2007) S300–S305. doi:10.1088/0964-1726/16/2/S15.

[6] G. Kovacs, L. During, Contractive tension force stack actuator based on soft dielectric eap, in: Proceedings of SPIE - The International Society for Optical Engineering, Vol. 7287, SPIE, 2009, p. 72870A. doi:10.1117/12.815195.

[7] G. Kofod, W. Wirges, M. Paajanen, S. Bauer, Energy minimization for self-organized structure formation and actuation, Applied Physics Letters 90 (8) (2007) 081916. doi:10.1063/1.2695785.

[8] O. A. Araromi, I. Gavrilovich, J. Shintake, S. Rosset, M. Richard, V. Gass, H. R. Shea, Rollable multisegment dielectric elastomer minimum energy structures for a deployable microsatellite gripper, IEEE/ASME Transactions on Mechatronics 20 (1) (2015) 438. doi:10.1109/TMECH.2014.2329367.

[9] M. Blum, M. Bueler, C. Graetzel, J. Giger, M. Aschwanden, Optotune focus tunable lenses and laser speckle reduction based on electroactive polymers, in: Proceedings of SPIE - The International Society for Optical Engineering, Vol. 8252, 2012, pp. 825207–825207–11. doi:10.1117/12.902631.

[10] S. J. Biggs, R. N. Hitchcock, Artificial muscle actuators for haptic displays: system design to match the dynamics and tactile sensitivity of the human fingerpad, in: Proceedings of SPIE - The International Society for Optical Engineering, Vol. 7642, 2010, pp. 76420I–76420I–12. doi:10.1117/12.847741.

[11] O. Araromi, P. Romano, S. Rosset, J. Perruisseau-Carrier, H. Shea, A tunable millimeter-wave phase shifter driven by dielectric elastomer actuators, in: Proceedings of SPIE, Vol. 9056, 2014, p. 90562M. doi:10.1117/12.2044589.

[12] J. Huang, T. Li, C. Chiang Foo, J. Zhu, D. R. Clarke, Z. Suo, Giant, voltage-actuated deformation of a dielectric elastomer under dead load, Applied Physics Letters 100 (4) (2012) 041911. doi:http://dx.doi.org/10.1063/1.3680591.

[13] T. Lu, J. Huang, C. Jordi, G. Kovacs, R. Huang, D. Clarke, Z. Suo, Dielectric elastomer actuators under equal-biaxial forces, uniaxial forces, and uniaxial constraint of stiff fibers, Soft Matter 8 (22) (2012) 6167–6173. doi:10.1039/c2sm25692d.

[14] S. Rosset, O. Araromi, H. Shea, Maximizing strain in miniaturized dielectric elastomer actuators, in: Proceedings of SPIE - The International Society for Optical Engineering, 2015.

[15] A. N. Gent, A new constitutive relation for rubber, Rubber Chemistry and Technology 69 (1) (1996) 59–61. doi:10.5254/1.3538357.

[16] L. Mullins, Softening of rubber by deformation, Rubber Chemistry and Technology 42 (1) (1969) 339–362. doi:10.5254/1.3539210.

[17] S. Rosset, L. Maffli, S. Houis, H. Shea, An instrument to obtain the correct biaxial hyperelastic parameters of silicones for accurate DEA modelling, in: Proceedings of SPIE - The International Society for Optical Engineering, Vol. 9056, 2014, p. 90560M. doi:10.1117/12.2044777.

[18] S. Rosset, M. Niklaus, V. Stojanov, A. Felber, P. Dubois, H. R. Shea, Ion-implanted compliant and patternable electrodes for miniaturized dielectric elastomer actuators, in: Proceedings of SPIE - The International Society for Optical Engineering, Vol. 6927, 2008, pp. 69270W–10. doi:10.1117/12.775727.

[19] S. Koh, C. Keplinger, T. Li, S. Bauer, Z. Suo, Dielectric elastomer generators: How much energy can be converted?, Mechatronics, IEEE/ASME Transactions on 16 (1) (2011) 33 –41. doi:10.1109/TMECH.2010.2089635.